iScience, Volume *26*

Supplemental information

Sex peptide regulates female receptivity through serotoninergic neurons in *Drosophila*

Yan Tong Yang, Shao Wei Hu, Xiaonan Li, Yuanjie Sun, Ping He, Kristi Anne Kohlmeier, and Yan Zhu

Figure S1

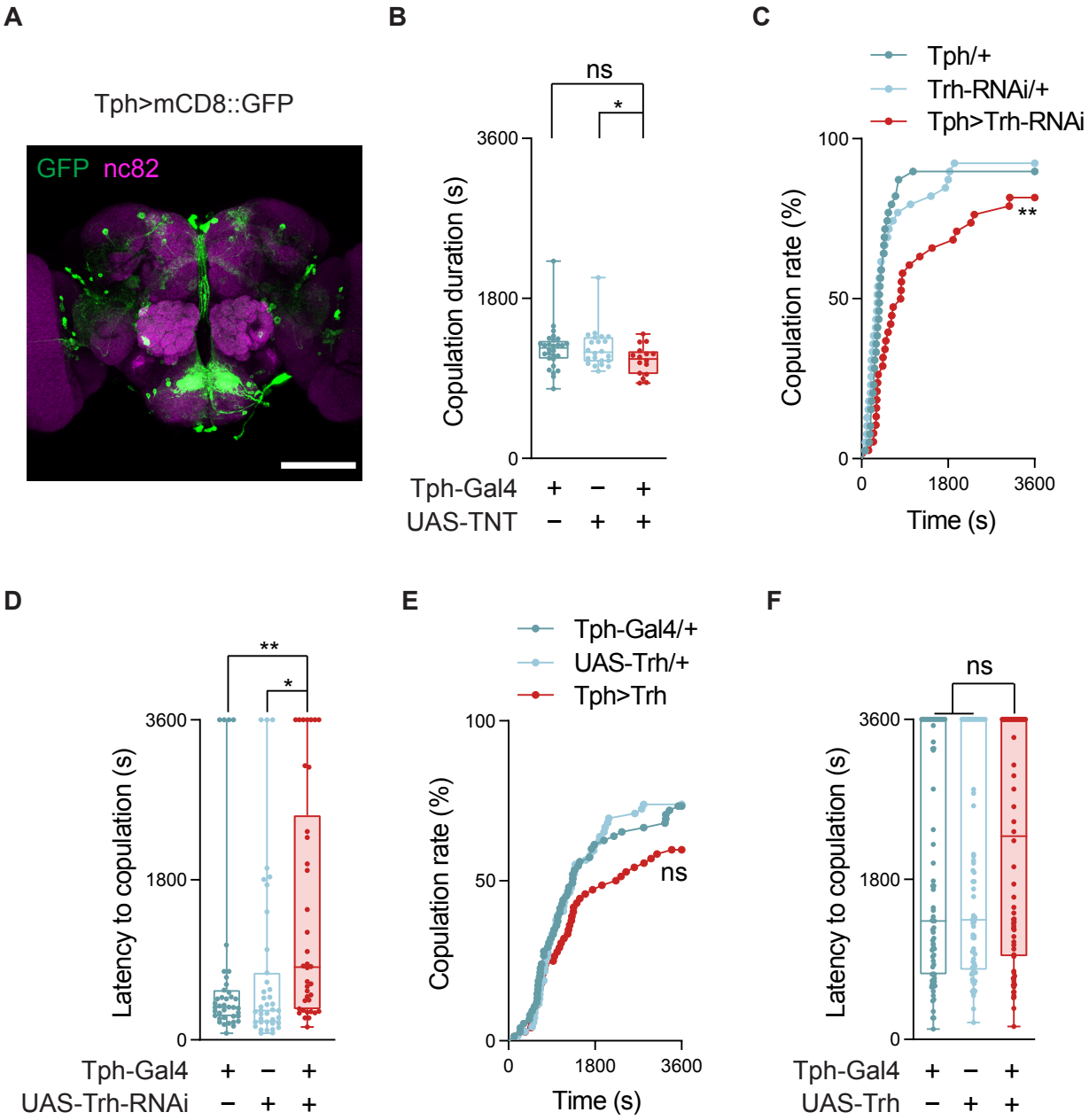
A
Tph>mCD8::GFP
GFP nc82
B
ns
*
3600
1800
0
Copulation duration (s)
Tph-Gal4 + − +
UAS-TNT − + +
C
Tph/+
Trh-RNAi/+
Tph>Trh-RNAi
100
50
0
Copulation rate (%)
**
0
1800
3600
Time (s)
D
**
*
3600
1800
0
Latency to copulation (s)
Tph-Gal4 + − +
UAS-Trh-RNAi − + +
E
Tph-Gal4/+
UAS-Trh/+
Tph>Trh
100
50
0
Copulation rate (%)
ns
0
1800
3600
Time (s)
F
ns
3600
1800
0
Latency to copulation (s)
Tph-Gal4 + − +
UAS-Trh − + +

Figure S2

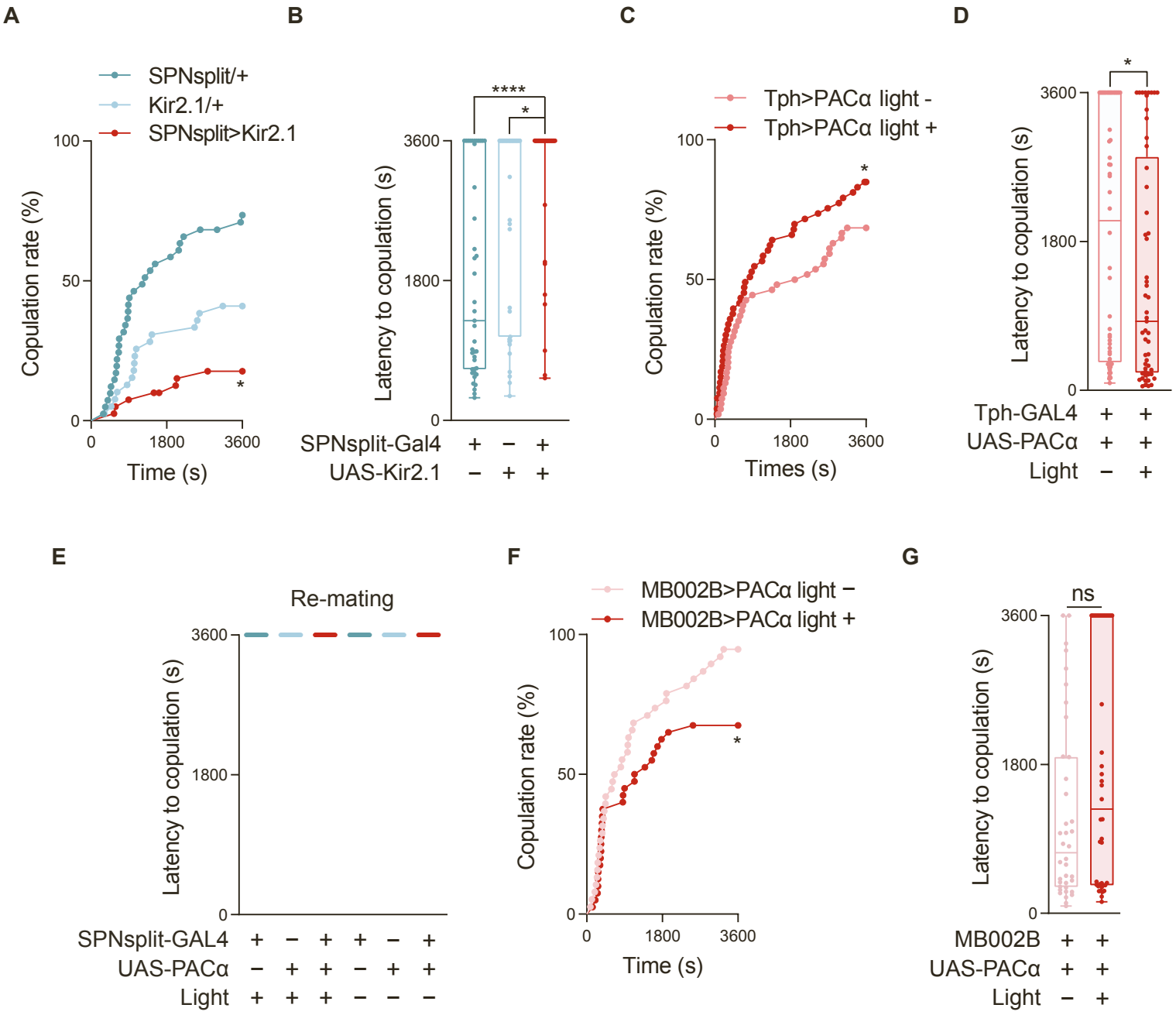
A
SPNsplit/+
Kir2.1/+
SPNsplit>Kir2.1
Copulation rate (%)
Time (s)
B
Latency to copulation (s)
SPNsplit-Gal4
UAS-Kir2.1
C
Tph>PACα light -
Tph>PACα light +
Copulation rate (%)
Times (s)
D
Latency to copulation (s)
Tph-GAL4
UAS-PACα
Light
E
Re-mating
Latency to copulation (s)
SPNsplit-GAL4
UAS-PACα
Light
F
MB002B>PACα light −
MB002B>PACα light +
Copulation rate (%)
Time (s)
G
ns
Latency to copulation (s)
MB002B
UAS-PACα
Light

Figure S3

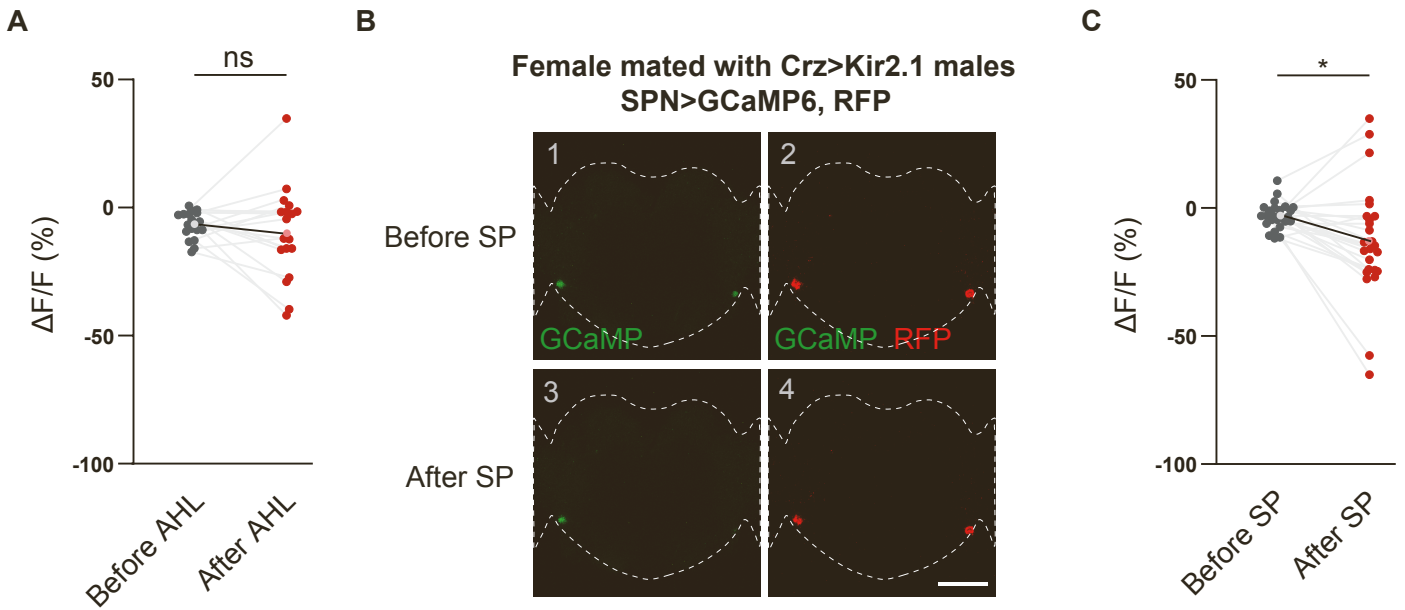
A
ns
50
0
-50
-100
ΔF/F (%)
Before AHL
After AHL
B
Female mated with Crz>Kir2.1 males
SPN>GCaMP6, RFP
Before SP
After SP
1
2
3
4
GCaMP
GCaMP RFP
C
*
50
0
-50
-100
ΔF/F (%)
Before SP
After SP

Figure S4

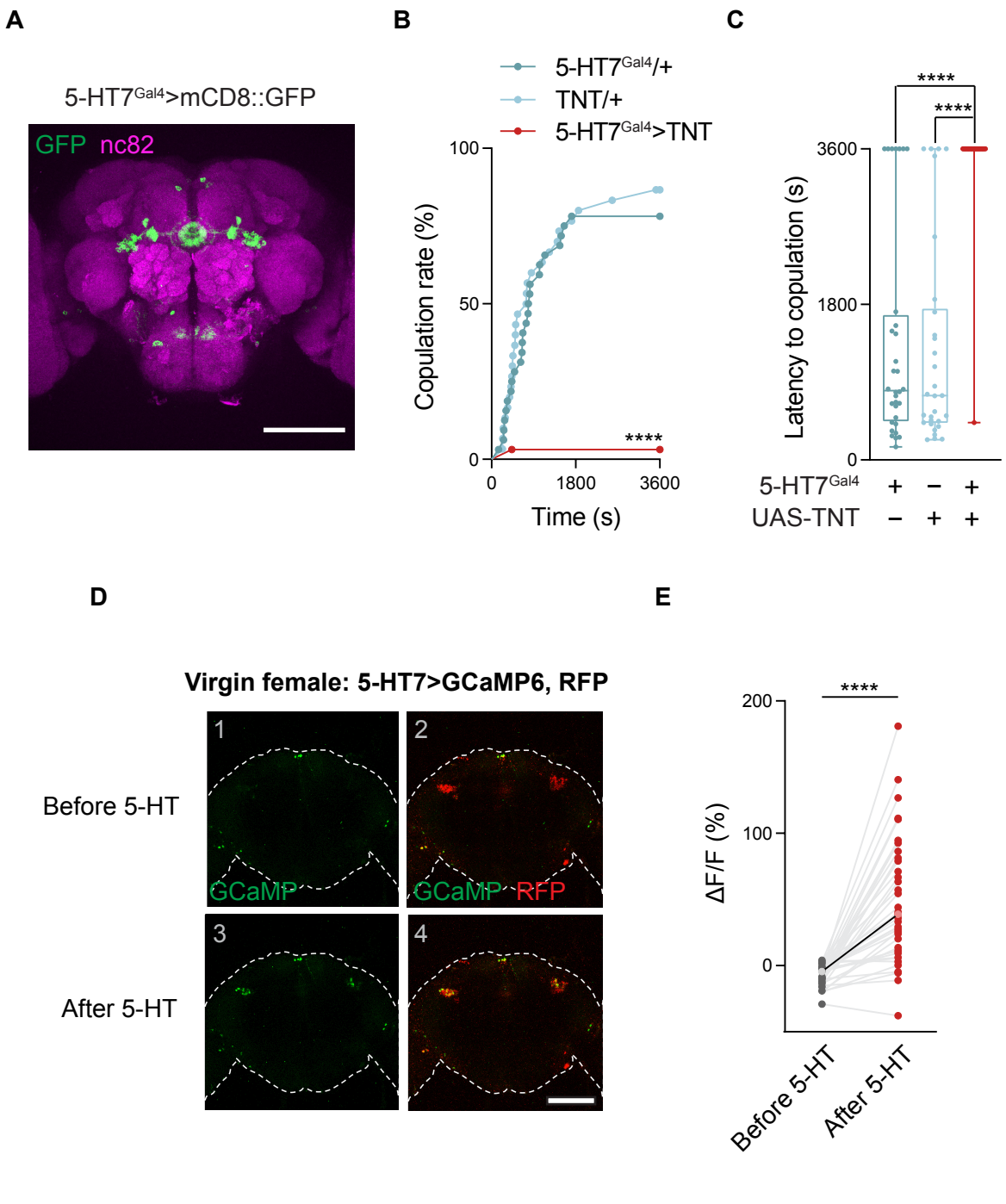
A
5-HT7Gal4>mCD8::GFP
GFP nc82
B
5-HT7Gal4/+
TNT/+
5-HT7Gal4>TNT
Copulation rate (%)
100
50
0
****
0
1800
3600
Time (s)
C
****
****
Latency to copulation (s)
3600
1800
0
5-HT7Gal4 + − +
UAS-TNT − + +
D
Virgin female: 5-HT7>GCaMP6, RFP
Before 5-HT
After 5-HT
1
2
3
4
GCaMP
GCaMP RFP
E
****
ΔF/F (%)
200
100
0
Before 5-HT
After 5-HT

Figure S5

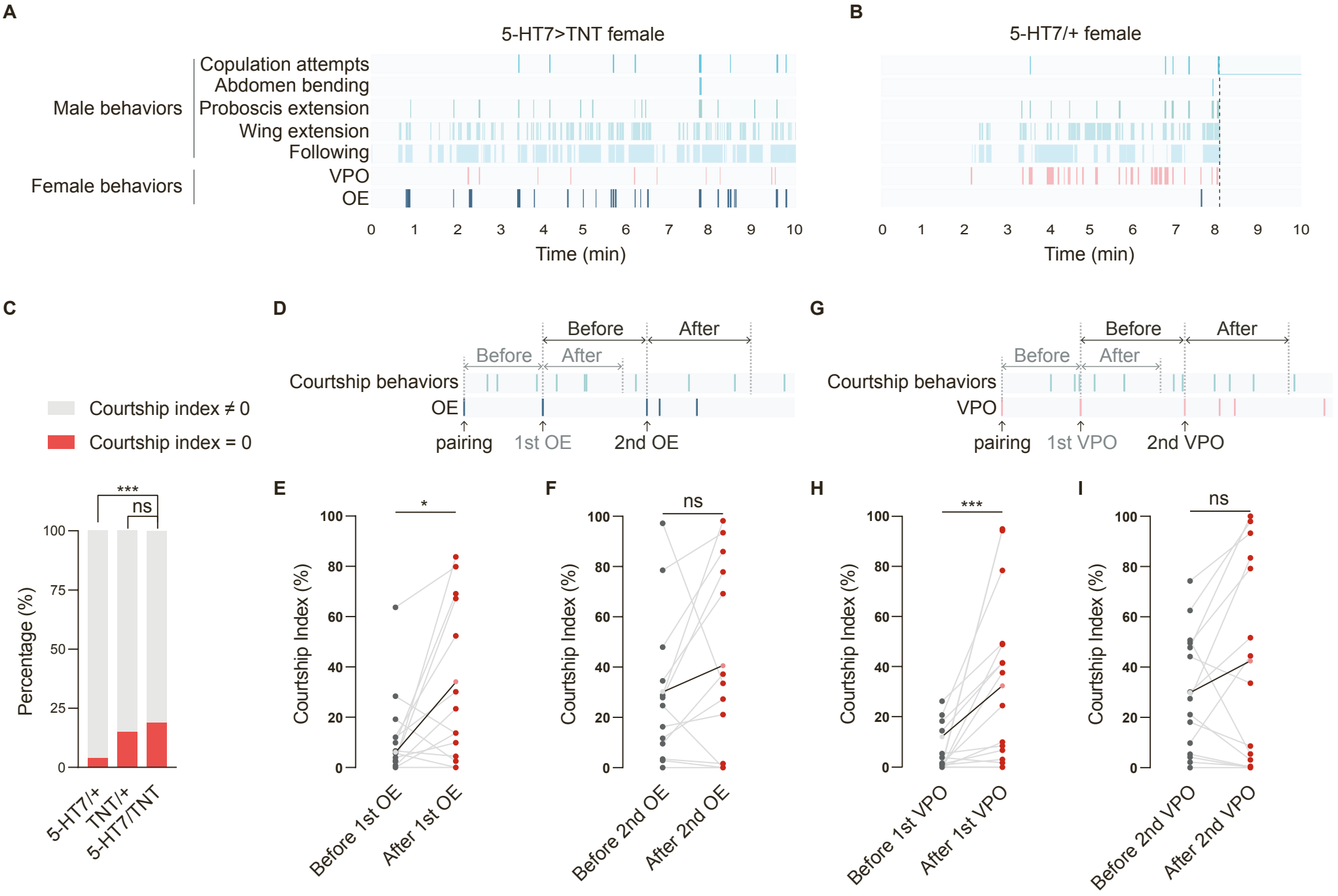
A
5-HT7>TNT female
Male behaviors
Copulation attempts
Abdomen bending
Proboscis extension
Wing extension
Following
Female behaviors
VPO
OE
0 1 2 3 4 5 6 7 8 9 10
Time (min)
B
5-HT7/+ female
0 1 2 3 4 5 6 7 8 9 10
Time (min)
C
Courtship index ≠ 0
Courtship index = 0
***
ns
Percentage (%)
100
75
50
25
0
5-HT7/+
TNT/+
5-HT7/TNT
D
Before
After
Before
After
Courtship behaviors
OE
pairing
1st OE
2nd OE
G
Before
After
Before
After
Courtship behaviors
VPO
pairing
1st VPO
2nd VPO
E
*
Courtship Index (%)
100
80
60
40
20
0
Before 1st OE
After 1st OE
F
ns
Courtship Index (%)
Before 2nd OE
After 2nd OE
H
***
Courtship Index (%)
Before 1st VPO
After 1st VPO
I
ns
Courtship Index (%)
Before 2nd VPO
After 2nd VPO

Figure S6

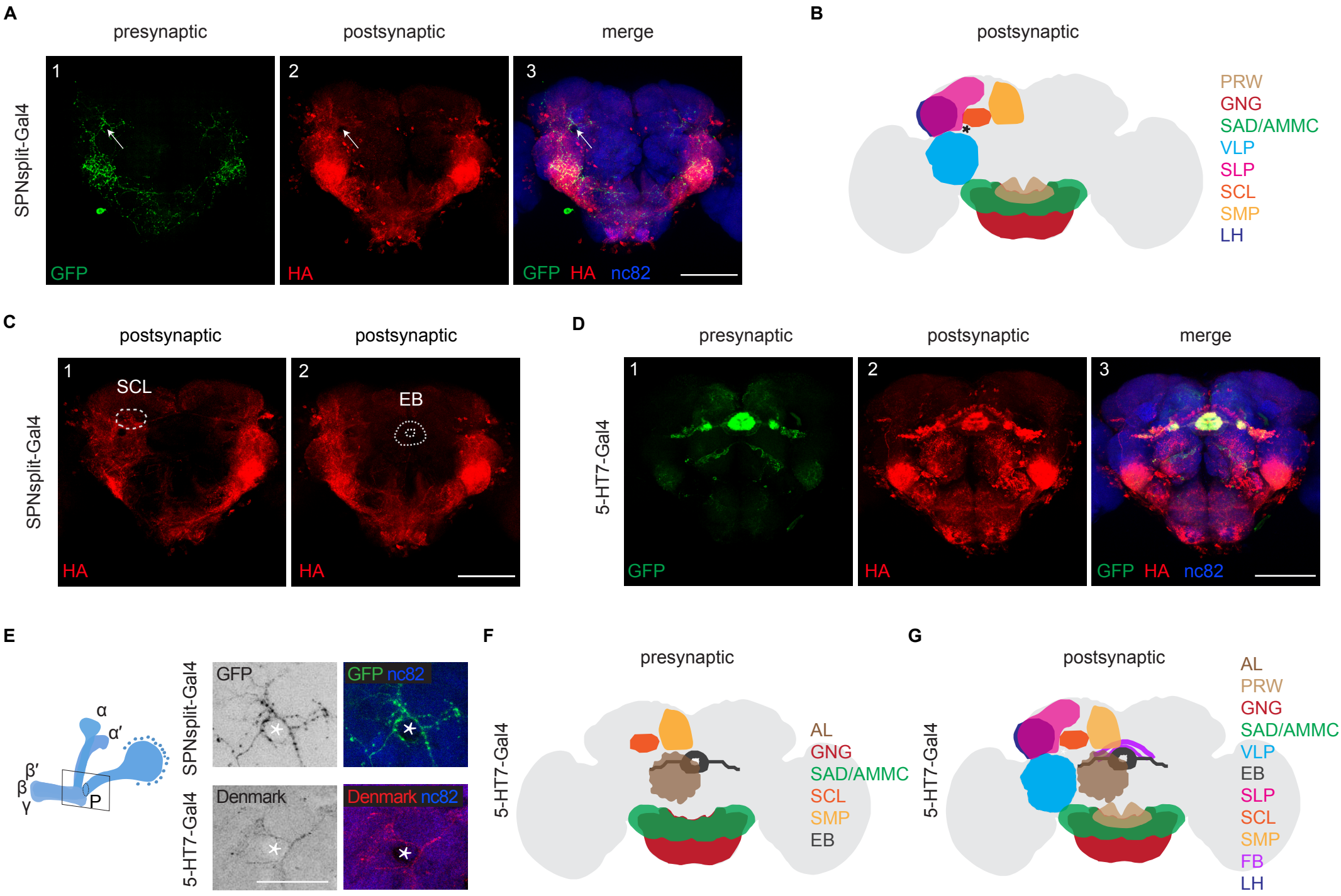
A
presynaptic
postsynaptic
merge
SPNsplit-Gal4
1
2
3
GFP
HA
GFP HA nc82
B
postsynaptic
PRW
GNG
SAD/AMMC
VLP
SLP
SCL
SMP
LH
C
postsynaptic
postsynaptic
SPNsplit-Gal4
SCL
EB
HA
HA
D
presynaptic
postsynaptic
merge
5-HT7-Gal4
GFP
HA
GFP HA nc82
E
α
α′
β′
β
γ
P
SPNsplit-Gal4
5-HT7-Gal4
GFP
GFP nc82
Denmark
Denmark nc82
F
presynaptic
5-HT7-Gal4
AL
GNG
SAD/AMMC
SCL
SMP
EB
G
postsynaptic
5-HT7-Gal4
AL
PRW
GNG
SAD/AMMC
VLP
EB
SLP
SCL
SMP
FB
LH

Figure S1. Serotonin is necessary for courtship receptivity in females, Related to Figure 1.

(A) Immunofluorescence of Tph neurons (green) in the brain of a *Tph-Gal4>UAS-mCD8::GFP* female.
(B) Comparison of the copulation durations of *Tph-Gal4>UAS-TNT* females and control females when paired with wild-type males (n = 16-28).
(C, D) Quantification of the copulation rate and latency to copulation in the pairs with a *Tph-Gal4>UAS-Trh*^{RNAi} female and a wild-type male (n = 38-39).
(E, F) Quantification of the copulation rate and latency to copulation in the pairs with a *Tph-Gal4>UAS-Trh* female and a wild-type male (n = 69-75).

All genotypes and experimental conditions are indicated with the plots. In the box-and-whisker plot, the whiskers mark the minimum and maximum, the box includes the 25th to 75th percentiles, and the line within the box indicates the median of the data set. The Kruskal–Wallis test was performed for (B), (D), and (F). The Log-Rank test was applied to (C) and (E), and among the statistical comparisons between the experimental group and controls, only the ones with less significance are shown. ns, not significant ($P \geq 0.05$); *$P < 0.05$; **$P < 0.01$. Scale bar in (A), 100 μm.

Figure S2. Subsets of 5-HT neurons are both necessary and sufficient for female sexual receptivity, Related to Figure 2.

(A, B) Quantification of the courtship events in pairs of a *SPNsplit-Gal4>UAS-Kir2.1* virgin female and wild-type male: the copulation rate (A) and latency to copulation (B) (n = 39-41).
(C, D) Quantification of the courtship events in pairs of a *Tph-Gal4>UAS-PACα* virgin female and a wild-type male: copulation rate (C) and latency to copulation (D) (n = 56-58).
(E) Quantification of the courtship outcomes in pairs of a mated female (genotype: *SPNsplit-Gal4>UA*S-PACα) and a wild-type male.
(F, G) Quantification of the courtship events in pairs of a *MB002B>UAS-PACα* virgin female and a wild-type male: copulation rate (E) and latency to copulation (F) (n = 38, 40).

All genotypes and experimental conditions are indicated with the plots. In the box-and-whisker plot, the whiskers mark the minimum and maximum, the box includes the 25th to 75th percentiles, and the line within the box indicates the median of the data set. The Log-Rank test was applied to (A), (C), and (E). In (A), among the statistical comparisons between the experimental group and controls, only the ones with less significance are shown. The Kruskal–Wallis test was performed for (B). The Mann-Whitney test was performed for (D) and (F). ns, not significant ($P \geq 0.05$); *$P < 0.05$; ****$P < 0.0001$.

Figure S3. Sex peptide decreased SPN neurons in females mated with SP-deficient males, Related to Figure 3.

(A) No change in fluorescence intensity of GCaMP6 signals in SPN neurons of female brains when treated with AHL alone (n = 18). The light gray and red dots indicate the mean of each data set.

(B) Representative images of SPN neurons responding to 60 μM SP treatment. The brains were from females mated with Crz > kir2.1 males. (B1-2): before treatment. (B3-4): after SP treatment. The genotype is *SPNsplit-Gal4>UAS-GCaMP6, UAS-myr::RFP*. The green channel indicates the GCaMP signals, and the red channel reveals the corresponding cell clusters. The dashed lines indicate the profiles of brains.

(C) Comparing the changes in normalized fluorescence intensity (ΔF/F) of GCaMP6 signals in SPN neurons of females mated with Crz > kir2.1 males, before and after SP treatment (n = 25). The light gray and red dots indicate the mean of each data set.

All genotypes and experimental conditions are indicated with the plots. The data points in (A) and (C) were jittered for a better view of overlapping data points. The paired t-test was performed for (A) and (C). ns, not significant ($P \geq 0.05$); *$P < 0.05$. In (B), the scale bars are 100 μm.

Figure S4. 5-HT7 neurons are necessary for sexual receptivity in females, Related to Figure 4.

(A) Immunofluorescence of 5-HT7 neurons (green) in a female of *5-HT7^{Gal4}>UAS-mCD8::GFP*.
(B, C) Quantification of the courtship events in pairs of a *5-HT7^{Gal4}>UAS-TNT* female and a wild-type male: copulation rate (H) and latency to copulation (I) (n = 30-32).
(D-E) Quantification of response of 5-HT7 neurons to the treatment of 5-HT.
(D) Representative images of GCaMP6 fluorescent signals in 5-HT7 neurons before (D1-2) and after (D3-4) the application of serotonin hydrochloride. Green indicates the GCaMP signals, and red labels the corresponding cell clusters. The genotype is *5-HT7-Gal4>UAS-GCaMP6, UAS-myr::RFP*. The dashed lines indicate the profiles of brains.
(E) Change of normalized fluorescence intensity (ΔF/F) of GCaMP6 signals in 5-HT7 neurons, after the treatment with serotonin hydrochloride (n = 39). The light gray and red dots indicate the mean of each data set.

All genotypes and experimental conditions are indicated with the plots. In the box-and-whisker plot, the whiskers mark the minimum and maximum, the box includes the 25th to 75th percentiles, and the line within the box indicates the median of the data set. The Log-Rank test was applied to (B), and among the statistical comparisons between the experimental group and controls, only the ones with less significance are shown. The Kruskal–Wallis test was performed for (C). The paired t-test was performed for (E). ****P < 0.0001.
In (A), nc82 (magenta) serves as a counterstaining. In (A) and (D), the scale bars are 100 μm.

Figure S5. Effects of VPO and OE behaviors from females on the motivation for courtship in the paired males, Related to Figure 5.

(A, B) Two examples of raster plots illustrating the bouts of OE (dark blue bars) and VPO (pink bars) in a *5-HT7>TNT* virgin female (A) and a *5-HT7/+* virgin female (B), together with various courtship behaviors (turquoise bars) of the paired wild-type males (*Canton S*). The vertical dash line in (B) indicates the start of copulation.

(C) Comparing the percentages of males displaying no courtship behaviors (red) when paired with different virgin females (*5-HT7>TNT* and genetic controls).

(D-F) Quantification of effects of OE from females with low sexual receptivity on male courtship motivation.

(D) Schema for defining a time period for each pair to quantify the combined male courtship behaviors before and after a specific female action event (first OE or second OE).

For each pair, the duration before the first OE is chosen as the latency from pairing to the first OE event, and the same length of time was also used as the duration after the first OE (light gray). Similarly, the duration before the second OE is the time interval between the first and the second OE, and this is also set as the duration after the second OE (dark gray).

(E, F) Comparing courtship indices of wild-type males before and after the first OE (E) or second OE (F) when paired with *5-HT7>TNT* females (n = 13, 14). The light gray and red dots indicate the mean of each data set.

(G-I) Quantification of effects of VPO from females with normal sexual receptivity on male courtship motivation.

(G) Schema for selecting a time period for each pair to quantify the combined male courtship behaviors before and after a specific female action event (first VPO or second VPO).

For each pair, the duration before the first VPO is chosen as the latency from pairing to the first VPO event, and the same length of time was also used as the duration after the first VPO (light gray). Similarly, the duration before the second VPO is the time interval between the first and the second VPO, and this is also set as the duration after the second VPO (dark gray).

(H, I) Comparing the courtship index of wild-type males before and after the first VPO (H) and second VPO (I) when paired with *5-HT7/+* females (n = 15, 16). The light gray and red dots indicate the mean of each data set.

In (D)-(I), the courtship index is the percentage of time a male spent showing courtship behaviors, including following, wing extension, proboscis extension, abdomen bending, and attempted copulation, toward the paired female over a specific time period. All genotypes and experimental conditions are indicated with the plots. The Chi-square test was performed for (C). The paired t-test was performed for (E), (F), (H), and (I). ns, not significant ($P \geq 0.05$); *$P < 0.05$; ***$P < 0.001$.

Figure S6. Exploring the synaptic connections between SPN and 5-HT7 neurons, Related to Figure 6.

(A) In flies bearing the SPNsplit-Gal4 and the *trans*-Tango components, the presynaptic expressions of ligand and myrGFP were driven by SPN neurons (A1, green), and postsynaptic signals were visualized in multiple brain regions as indicated (A2, red). nc82 (blue) serves as a counterstaining. The white arrows indicate the location of MB peduncle.
(B) Illustration of the brain regions receiving SPN projections. The dark asterisk indicates the location of MB peduncle.
(C) Showing the postsynaptic areas of SPN in the superior clamp surrounding the MB peduncle (C1), and the absence of postsynaptic signal in the areas surrounding EB (C2). The dashed lines indicate the corresponding brain regions.
(D) In flies bearing the *trans*-Tango components, 5-HT7-Gal4 drove the presynaptic expressions of ligand and myrGFP (D1, green) and generated massively postsynaptic signals throughout the brain (D2, red). nc82 (blue) serves as a counterstaining.
(E) Left: 3D model showing the structure of the mushroom body. The dashed circle indicates the site on the peduncle to be imaged; the rectangle indicates the imaging frame. Right: enlarged views to show the signal of SPNsplit-Gal4 (top) and 5-HT7-Gal4 (bottom) labeled neurons near and surrounding the MB peduncle. The white asterisks indicate the location of the peduncle. nc82 (blue) serves as a counterstaining.
(F) Illustration of the brain regions with presynaptic expressions in flies bearing 5-HT7-Gal4 and the *trans*-Tango components.
(G) Illustration of the brain regions receiving 5-HT7 projections.

In (B), (F), and (G), the abbreviations of the indicated areas: antenna lobe (AL), antennal mechanosensory and motor center (AMMC), ellipsoid body (EB), fan-shaped body (FB), gnathal ganglia (GNG), lateral horn (LH), prow (PRW), saddle (SAD), the superior clamp (SCL), the superior lateral protocerebrum (SLP), superior medial protocerebrum (SMP) and the ventral-lateral protocerebrum (VLP). In (A) and (D), the signals from a stack of confocal images of the whole brain were shown. In (C) and (E), only the signals from the relevant imaging layers of the brain were shown. Scale bar for (A), (C), and (D) are 100 μm, for (E) is 50 μm.